DISTRIBUTION STATEMENT A: Approved for public release; distribution is unlimited.

Data Analysis, Modeling, and Ensemble Forecasting to Support NOWCAST and Forecast Activities at the Fallon Naval Station

Darko Koracin
Desert Research Institute
2215 Raggio Parkway, Reno, NV 89512
phone: (775) 674-7091 fax: (775) 674-7016 email: Darko.Koracin@dri.edu

John Lewis
Desert Research Institute
2215 Raggio Parkway, Reno, NV 89512
phone: (775) 674-7077 fax: (775) 674-7016 email: John.Lewis@dri.edu

Grant Number: N00014-08-1-0451
http://www.adim.dri.edu/

LONG-TERM GOALS

The goals of this project are to increase our understanding of weather predictability and its advantages and limitations, and to develop methods to provide more accurate forecasts and nowcasts in complex terrain using multi-model ensemble modeling techniques and special observations including remotely sensed data.

OBJECTIVES

The main objectives of the study are: 1) to further develop, test, and continue twice daily operational forecasts using both the real time Weather and Research Forecasting (WRF Version 3.2) model (Skamarock et al. 2008) and Mesoscale Model 5 (MM5 Version 3.7.2) (Grell et al. 1994) with sub-kilometer horizontal resolution to support the NOWCAST system at the Fallon Naval Air Station (NAS); 2) To assess multi-model ensemble forecasting capabilities and to subsequently include forecasts as a part of a multi-model ensemble using WRF, MM5, and the Coastal Oceanic and Atmospheric Modeling Prediction System (COAMPS^{TM}, Vesion 3.1.1); 3) To develop methods that combine multi-model ensemble forecasts with climatological fields to improve the skill of the forecasts and nowcasts; and 4) To develop a framework that complements the ensemble forecasting to better understand the sources of error and uncertainty in dynamical forecasts relevant to nowcasting key parameters such as wind speed, cloud fields, and visibility over the Fallon NAS area.

APPROACH

This project broadly focuses on the following components: (1) maintenance and data collection, quality control, and analysis of data from four special weather stations in the Fallon Naval Air Station area; (2) development of a regional/mesoscale multi-model (COAMPS^{TM}, WRF, and MM5) ensemble

forecasting system. The ensemble members for MM5 and WRF are generated by selecting different choices of physical parameterizations (planetary boundary layer (PBL) schemes, cumulus convection schemes, explicit cloud microphysical schemes, and radiation schemes) of each model, and perturbations of initial and boundary conditions (IC/BCs) following Stensrud et al. (2000), Stensrud (2001), and Stensrud and Weiss (2002). Ensemble experiments were conducted on a 36 km grid (shown in Fig. 1) nested into a 108 km grid that covers the entire North American continent and adjoining Pacific Ocean. The main objective is to obtain meaningful probability density functions (pdfs) for medium-to-long-range forecasting (from a week to 2 weeks) of the forecast variables; that is, to create and analyze pdfs for variables from each model and then combine the models (three-model ensemble) with a total of 150 ensemble members generated from altering the physics options. The second experiment includes 100 WRF ensemble members generated through perturbations of initial/lateral boundary conditions. In addition, high-resolution control runs (12 km grid) served as a valuable means of comparison with the ensemble results (Houtekamer and Mitchell 1999); (3) development of dynamic data assimilation methods that have duality with 4D-VAR (four-dimensional variational assimilation) to understand the sensitivity of the model forecast control elements and to reduce the forecast error; and (4) analyzing the models' skill in determining the likelihood of intense wind and gusty conditions at the NAS through synoptic and sub-synoptic scale dynamic signatures.

WORK COMPLETED

The skill of the multi-model ensemble forecast products were analyzed based on: (a) statistical verification to estimate the skill scores, (b) pdf diagnosis, statistics, and evolution; (c) rank histograms (Talagrand diagrams); and (d) Evolution and spread of parameter trajectories ("spaghetti plots": Superposition of forecast isolines for the ensemble members).

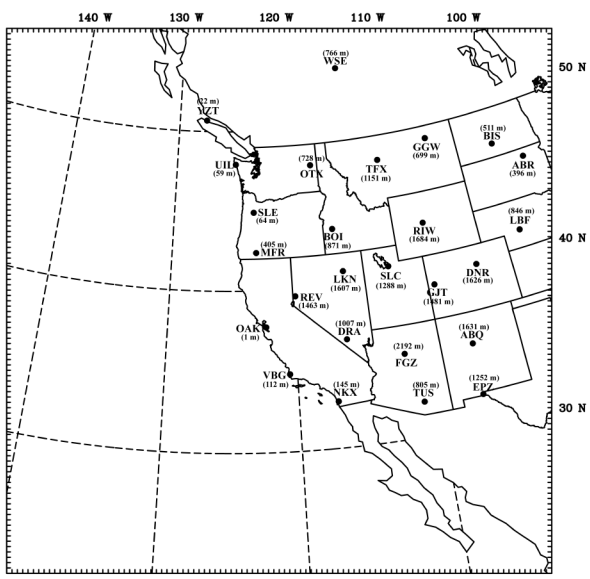

Figure 1. MM5, WRF, and COAMPS^{TM} nested modeling domain (horizontal grid resolution = 36 km). Black dots indicate the locations of radiosonde stations used in the analysis. Station elevations (mean sea level) are shown in parentheses.

The main ensemble technique was developed for MM5 and WRF using a sufficient set of physics parameterization options that are available (Table 1). The physics options consisted of a variety of PBL schemes, single and double-moment cloud microphysics, simple to complex radiation and cumulus parameterization schemes. We have made a total of 100 ensemble forecasts for a period of 15 days (12-27 December 2008) with 50 members randomly drawn from each of WRF and MM5. At this point, we were able to add an initial set of 50 COAMPS^{TM} model runs; however, the COAMPS runs are only a preliminary set since we did not have the newest version which would allow much richer selection of physics options. The preliminary COAMPS ensemble run settings include two boundary layer parameterization schemes following Mellor and Yamada, four ice nucleation types, three mixing length schemes, and two autoconversions of cloud water parameters. We are communicating with NRL to improve the COAMPS ensemble set. The simulated case period was chosen because of the two intense frontal passages that occurred over NW Nevada. The initial and boundary conditions for MM5 and WRF were retrieved from the NCEP's Global Forecast System (GFS; http://www.emc.ncep.noaa.gov/). The Navy Operational Global Atmospheric Prediction System NOGAPS 4.0 (archived on 54 km grid; Bayler and Lewit 1992) forecast products were used as the initial analysis fields for COAMPS^{TM} .

Table 1. Ensemble set of physical parameterizations in MM5 and WRF.

Experiment	*MM5 (PBL)*	*MM5 (Microphysics)*	*MM5 (Cumulus)*	*MM5 (Radiation)*	*WRF (PBL)*	*WRF (Microphysics)*	*WRF (Cumulus)*	*WRF (Radiation)*
Control	Eta M-Y	Reisner 2	Kain-Fritsch	RRTM (FRAD=4)	Mellor-Yamada-Jan	Thompson	Kain-Fritsch	Dudhia/RRTM
1	Eta M-Y	Reisner 2	Grell	CCM2 (FRAD=3)	Mellor-Yamada-Jan	Goddard microphysics	Betts-Miller	GFDL/GFDL
2	Eta M-Y	Simple ice (Dudhia)	Grell	Dudhia (FRAD=2)	Mellor-Yamada-Jan	Goddard microphysics	Kain-Fritsch	GFDL/GFDL
3	Eta M-Y	Goddard (GFSC)	Grell	Dudhia (FRAD=2)	Mellor-Yamada-Jan	Lin	Kain-Fritsch	Goddard/RRTM
4	Eta M-Y	Reisner 2	Betts-Miller	CCM2 (FRAD=3)	Mellor-Yamada-Jan	Eta microphysics	Kain-Fritsch	GFDL/GFDL
5	Eta M-Y	Reisner 2	Grell	Dudhia (FRAD=2)	Mellor-Yamada-Jan	Eta microphysics	Betts-Miller	CAM/CAM
6	Eta M-Y	Schultz	Betts-Miller	Dudhia (FRAD=2)	Mellor-Yamada-Jan	Eta microphysics	Kain-Fritsch	CAM/CAM
7	Eta M-Y	Simple ice (Dudhia)	Grell	CCM2 (FRAD=3)	Mellor-Yamada-Jan	Thompson	Betts-Miller	Dudhia/RRTM
8	Eta M-Y	Goddard (GFSC)	Betts-Miller	Dudhia (FRAD=2)	Mellor-Yamada-Jan	Goddard microphysics	Grell-Devenyi	GFDL/GFDL
9	Eta M-Y	Reisner (no graupel)	Kain-Fritsch	Simple cloud (FRAD=1)	Mellor-Yamada-Jan	Goddard microphysics	Betts-Miller	CAM/CAM
10	Eta M-Y	Reisner 2	Betts-Miller	RRTM (FRAD=4)	Mellor-Yamada-Jan	Thompson	Betts-Miller	CAM/CAM
11	Eta M-Y	Simple ice (Dudhia)	Betts-Miller	Dudhia (FRAD=2)	Mellor-Yamada-Jan	Thompson	Betts-Miller	Goodard/RRTM
12	Eta M-Y	Simple ice (Dudhia)	Betts-Miller	CCM2 (FRAD=3)	Mellor-Yamada-Jan	Lin	Grell-Devenyi	Goddard/RRTM
13	Gayno-Seaman	Schultz	Betts-Miller	CCM2 (FRAD=3)	Mellor-Yamada-Jan	Lin	Betts-Miller	GFDL/GFDL
14	Gayno-Seaman	Goddard (GFSC)	Betts-Miller	CCM2 (FRAD=3)	Mellor-Yamada-Jan	Goddard microphysics	Betts-Miller	GFDL/RRTM
15	Gayno-Seaman	Reisner 2	Grell	Dudhia (FRAD=2)	Mellor-Yamada-Jan	Lin et	Kain-Fritsch	Dudhia/GFDL
16	Blackadar	Schultz	Kain-Fritsch	RRTM (FRAD=4)	Mellor-Yamada-Jan	Eta microphysics	Kain-Fritsch	Dudhia/CAM
17	Gayno-Seaman	Reisner 2	Betts-Miller	CCM2 (FRAD=3)	Mellor-Yamada-Jan	WRF-single mom (6)	Betts-Miller	Goddard/RRTM
18	Blackadar	Simple ice (Dudhia)	Grell	Dudhia (FRAD=2)	Mellor-Yamada-Jan	WRF-single mom (3)	Kain-Fritsch	Dudhia/RRTM
19	Gayno-Seaman	Goddard (GFSC)	Grell	Simple cloud (FRAD=1)	Mellor-Yamada-Jan	Morrison	Kain-Fritsch	Goddard/RRTM
20	Gayno-Seaman	Schultz	Kain-Fritsch	Dudhia (FRAD=2)	Mellor-Yamada-Jan	Morrison	Betts-Miller	Goddard/RRTM
21	Gayno-Seaman	Simple ice (Dudhia)	Grell	CCM2 (FRAD=3)	Mellor-Yamada-Jan	Morrison	Grell-Devenyi	Goddard/RRTM
22	Gayno-Seaman	Goddard (GFSC)	Kain-Fritsch	Simple cloud (FRAD=1)	YSU (new MRF)	Eta microphysics	Kain-Fritsch	GFDL/GFDL
23	Gayno-Seaman	Simple ice (Dudhia)	Kain-Fritsch	RRTM (FRAD=4)	YSU (new MRF)	Lin	Betts-Miller	GFDL/GFDL
24	Gayno-Seaman	Goddard (GFSC)	Grell	Dudhia (FRAD=2)	YSU (new MRF)	Goddard microphysics	Betts-Miller	Goddard/RRTM
25	Gayno-Seaman	Goddard (GFSC)	Kain-Fritsch	CCM2 (FRAD=3)	YSU (new MRF)	Lin	Kain-Fritsch	CAM/CAM
26	Gayno-Seaman	Goddard (GFSC)	Betts-Miller	RRTM (FRAD=4)	YSU (new MRF)	Lin	Betts-Miller	CAM/CAM
27	Gayno-Seaman	Simple ice (Dudhia)	Kain-Fritsch	Simple cloud (FRAD=1)	YSU (new MRF)	Goddard microphysics	Betts-Miller	Dudhia/RRTM
28	Blackadar	Schultz	Kain-Fritsch	CCM2 (FRAD=3)	YSU (new MRF)	Thompson	Grell-Devenyi	GFDL/GFDL
29	Gayno-Seaman	Reisner 2	Kain-Fritsch	Simple cloud (FRAD=1)	YSU (new MRF)	Eta microphysics	Betts-Miller	Goddard/RRTM
30	Burk-Thompson	Reisner 2	Betts-Miller	Simple cloud (FRAD=1)	YSU (new MRF)	Eta microphysics	Kain-Fritsch	CAM/CAM
31	Burk-Thompson	Simple ice (Dudhia)	Betts-Miller	Simple cloud (FRAD=1)	YSU (new MRF)	Morrison	Kain-Fritsch	Goddard/RRTM
32	Burk-Thompson	Reisner 2	Kain-Fritsch	Dudhia (FRAD=2)	YSU (new MRF)	WRF-single mom(6)	Kain-Fritsch	Goddard/RRTM
33	Burk-Thompson	Reisner 2	Betts-Miller	RRTM (FRAD=4)	YSU (new MRF)	WRF-single mom(3)	Betts-Miller	Dudhia/RRTM
34	Burk-Thompson	Simple ice (Dudhia)	Betts-Miller	RRTM (FRAD=4)	YSU (new MRF)	WRF-single mom(6)	Betts-Miller	CAM/CAM
35	Burk-Thompson	Reisner 2	Betts-Miller	Dudhia (FRAD=2)	Pleim-Xiu	Eta microphysics	Betts-Miller	Goddard/RRTM
36	Burk-Thompson	Goddard (GFSC)	Grell	CCM2 (FRAD=3)	Pleim-Xiu	Lin	Betts-Miller	Goddard/RRTM
37	Burk-Thompson	Simple ice (Dudhia)	Betts-Miller	CCM2 (FRAD=3)	Pleim-Xiu	Eta microphysics	Grell-Devenyi	GFDL/GFDL
38	Burk-Thompson	Schultz	Betts-Miller	Dudhia (FRAD=2)	Pleim-Xiu	Goddard microphysics	Grell-Devenyi	Dudhia/RRTM
39	Burk-Thompson	Reisner 2	Kain-Fritsch	Simple cloud (FRAD=1)	Pleim-Xiu	Lin	Kain-Fritsch	GFDL/GFDL
40	Burk-Thompson	Goddard (GFSC)	Kain-Fritsch	Simple cloud (FRAD=1)	Pleim-Xiu	Thompson	Kain-Fritsch	GFDL/GFDL
41	MRF	Reisner 2	Kain-Fritsch	Dudhia (FRAD=2)	Pleim-Xiu	Goddard microphysics	Grell-Devenyi	CAM/CAM
42	MRF	Simple ice (Dudhia)	Betts-Miller	Dudhia (FRAD=2)	Pleim-Xiu	Goddard microphysics	Kain-Fritsch	CAM/CAM
43	MRF	Reisner 2	Grell	CCM2 (FRAD=3)	Pleim-Xiu	WRF-single mom(6)	Kain-Fritsch	Goddard/RRTM
44	MRF	Reisner 2	Kain-Fritsch	RRTM (FRAD=4)	Pleim-Xiu	Morrison	Kain-Fritsch	Goddard/RRTM
45	MRF	Schultz	Grell	CCM2 (FRAD=3)	Pleim-Xiu	Lin et al.	Kain-Fritsch	CAM/CAM
46	MRF	Schultz	Betts-Miller	RRTM (FRAD=4)	Pleim-Xiu	Goddard microphysics	Betts-Miller	Dudhia/RRTM
47	MRF	Simple ice (Dudhia)	Kain-Fritsch	RRTM (FRAD=4)	Pleim-Xiu	Lin	Betts-Miller	Dudhia/RRTM
48	MRF	Goddard (GFSC)	Betts-Miller	RRTM (FRAD=4)	Pleim-Xiu	Lin	Grell-Devenyi	Dudhia/RRTM
49	MRF	Simple ice (Dudhia)	Grell	CCM2 (FRAD=3)	Pleim-Xiu	Goddard microphysics	Grell-Devenyi	Dudhia/RRTM
50	MRF	Simple ice (Dudhia)	Grell	Dudhia (FRAD=2)	Pleim-Xiu	Lin	Kain-Fritsch	GFDL/GFDL

The second numerical experiment included an additional 100 WRF ensemble members that were generated by random perturbations of the GFS initial and boundary conditions using the WRF-3D-VAR module (Barker et al. 2004). As an example, the perturbation distributions for the temperature, relative humidity, and winds at 500 hPa for ensemble member 1 on the 36 km grid are shown in Figure 2. The absolute values of the perturbations at 500 hPa are generally $3^{o}C$ for temperature , 30% for relative humidity and 4 m s^{-1} for the components of wind field. Verification was carried out using data from 29 upper air sounding locations (Fig. 1). A statistical verification is carried out using 15-day forecasts of temperature, geopotential height, and winds.

To understand the sources of forecast errors in the dynamical models, we have developed a dynamic data assimilation method that has combined the variational analysis with model sensitivity tests (Lakshmivarahan and Lewis 2010). The method has been proven to be equivalent to 4D-VAR (the four-dimensional variational assimilation method) but with added information on the sensitivity of the model forecast to the elements of control (initial conditions, boundary conditions, and physical/empirical parameters). The optimal state of control is found through the solution to an inversion problem, i.e., a solution of **A**x=b where A is a matrix related to the sensitivities, b is the forecast error at the times/locations of the observations and x is the optimal changes to control that minimize the forecast error. The advantage of this approach over traditional 4D-VAR stems from an ability to reduce forecast error through knowledge of the sensitivity that can be used to determine the placement of observations of each forecasted variable. The primary disadvantage is that calculation of the time evolution of sensitivity significantly adds to the computational burden. Thus, it is not designed as a replacement for operational 4D-VAR, rather it is ideally suited for identifying the sources of systematic errors in dynamical models and for idealized placement of observations to reduce the forecast error.

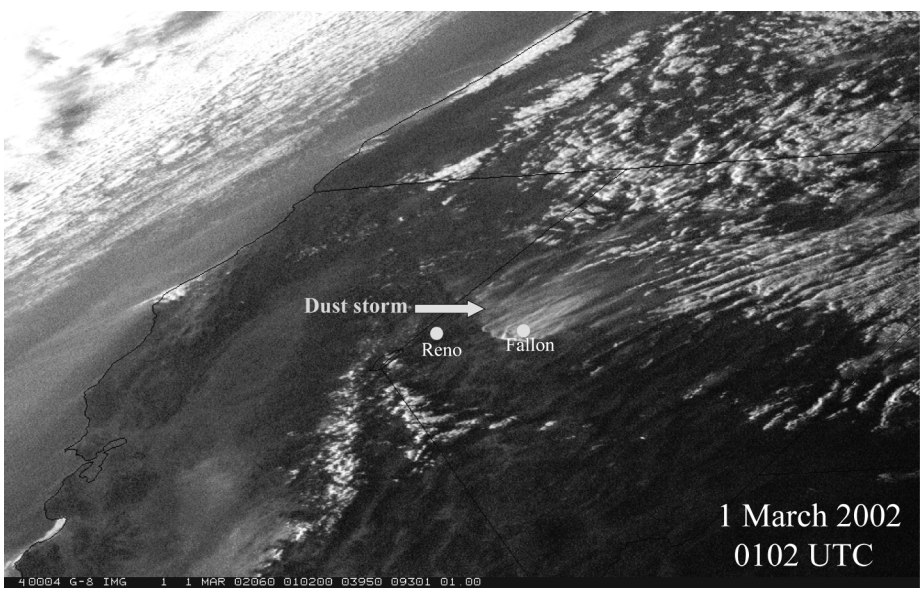

Figure 2. GOES-8 satellite imagery of cloud and dust valid at 0102 UTC (03/01/2002). Locations of Fallon and Reno are indicated in the figure.

We have conducted a study of forecasting restricted visibility at Fallon NAS in response to a dust storm that formed over the Black Rock Desert (BRD) of northwestern Nevada and spread southwards to impact operations at the NAS. Two studies have been completed for the dust storm of February/March 2002 (the satellite imagery of the dust storm is shown in Fig. 2). The first study identified large-scale dynamic signatures linked to the storm, and the second study used the WRF model to simulate smaller scale processes associated with the storm.

RESULTS

The behavior of the spatial and temporal characteristics of the multi-model ensemble forecasts is analyzed using the isoline patterns and forecast trajectories of particular parameters such as the geopotential height and temperature simulated from each ensemble forecast member. An illustration of the MM5 and WRF ensemble members simultaneous with the preliminary COAMPS runs is shown in Fig. 3.

The MM5 and WRF ensemble members closely followed the frontal passage when the dynamics were active and showed less dependence on physical parameterizations to produce adequate ensemble spread during the first two days of the predictions. During the 2-5 day forecast period, MM5 and WRF showed a bimodal split in the forecast trajectories, and for the subsequent period the spread in the trajectories is similar. WRF ensemble members generally showed good correspondence with the observations for a forecast period of about 7 days; the influence of the physics schemes is more significant in the lower levels than aloft. It is to be noted that none of the models reproduced the second cold advection (25 Dec 2008) during the end of the forecast period. In part, this is due to the impact of the boundary conditions coming from the GFS fields. It is also to be noted that the GFS forecasts have had a similar forecast trend, as seen in MM5 and WRF during the end of forecast period, and the spatial resolution of GFS (2.5° × 2.5°) is also apparently sensitive while employing the GFS boundary conditions for MM5 and WRF. There is no distinct trend in the spread of forecast trajectories at different pressure levels. The final statistics will be computed when the ensemble runs with the newest COAMPS version and physics options will be completed.

With the application of the WRF-3D-VAR module, random perturbations for initial conditions (ICs) were created based on randomly choosing values from the standard normally distributed function. The ensemble simulations of WRF used two modeling domains (1: 108 km grid and 2: 36 km grid shown in Fig. 1), the ensemble runs were conducted with the ICs' perturbation for domain 1 and domain 2 separately, in order to shed light on the influence of the domain size, the perturbation of ICs and the lateral boundary conditions (LBCs) on the spread of the ensemble. The perturbation distributions of ensemble member 1 for the modeling domains 1 (108 km grid) and 2 (36 km grid; shown in Fig. 1) are shown in Figures 4 and 5, respectively. The perturbation of temperature for coarser domain 1 is from -3 ^{o}C to 2.5 ^{o}C, for relative humidity is from -30 % to 25 %, for wind component U-component of wind is from -3 m/s to 2.5 m/s, and for V-component of wind is from -4 m/s to 3 m/s. As for domain 2, the amplitude of the perturbation for temperature is 2.5 ^{o}C, 3 m/s for U component of wind, and 4 m/s for V-component of wind.

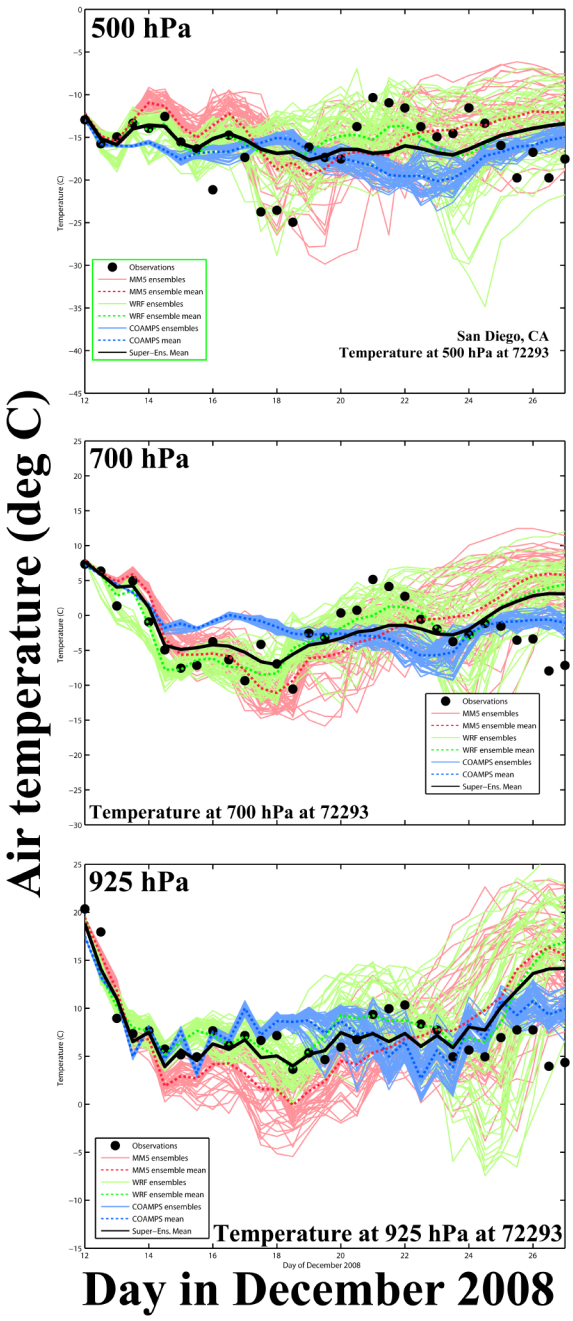

Figure 3. COAMPS^{TM} (blue), MM5 (red), and WRF (green) ensemble trajectories for the air temperature at San Diego, CA, at 500 (upper), 700 (middle), and 925 (lower row) hPa with superimposed radiosonde observations (heavy black dots) for the period from 12 to 27 December 2008.

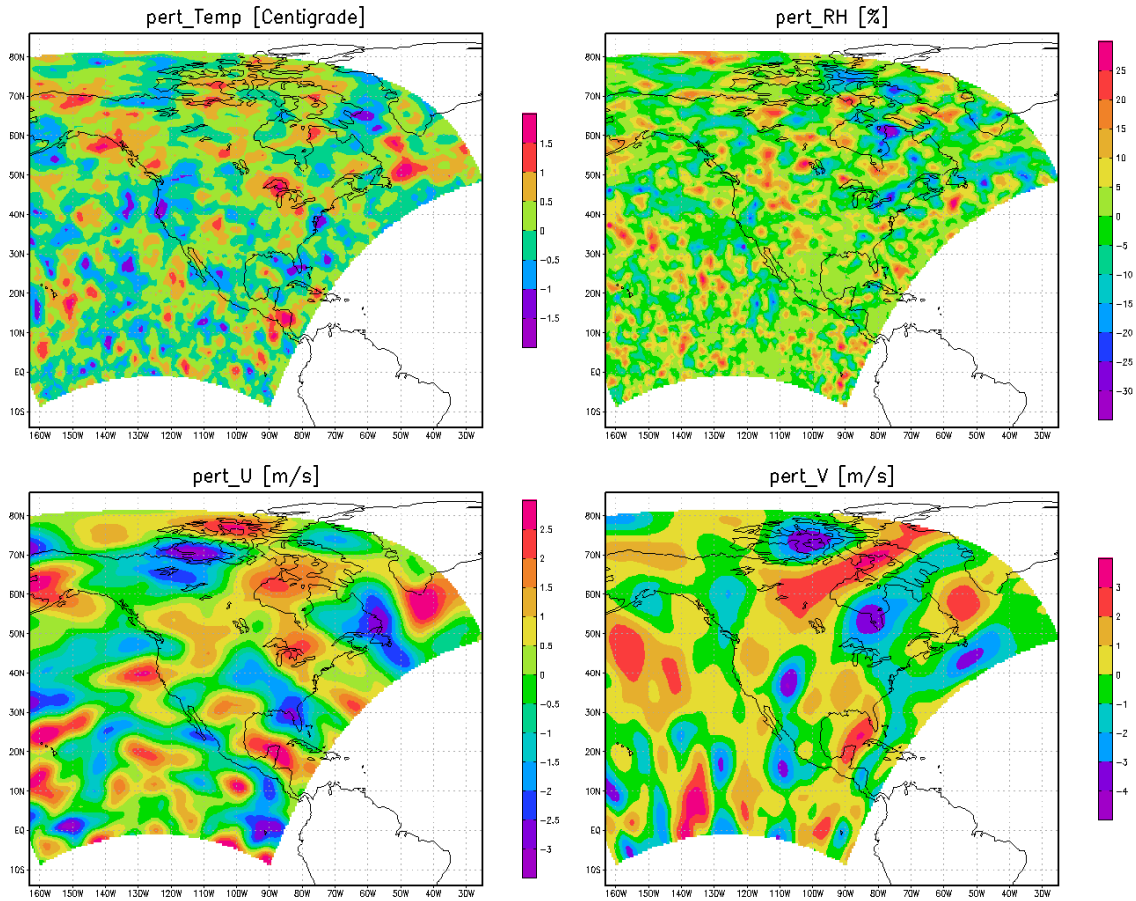

Figure 4. Perturbation distribution for temperature and relative humidity, and components of wind at 500hPa on the modeling domain (108 km grid), valid at 00 UTC 12 December 2008.

Figure 6 show the forecast trajectories of the 500 hPa air temperatures at Oakland, CA from the ensemble set by perturbation of ICs only. It is seen that the ICs' perturbation on a larger domain size (left panels of Fig. 6; a domain size covering the entire North American continent) maintained the ensemble spread for the entire forecasting range of 15 days, whereas the spread rapidly decayed for smaller domain size (right panel of Fig. 6) after 2 days of the forecasting. If errors propagate inward from the lateral boundaries at a speed of 20-30° longitude per day, the lateral boundary conditions are more important for smaller domain sizes (Baumhefner and Perkey 1982). Ensemble experiments with perturbations of lateral boundary conditions (LBCs) on the smaller domain size (domain shown in Fig. 1) showed significant ensemble spread in this case. Table 2 shows the statistics using RMSE (root mean square error), bias, sd-bias (bias of standard deviation) and dispersion for the WRF control run, the mean of the ensemble with perturbations of ICs' on larger domain sizes (50 members), and the mean of the ensemble with the ICs' and LBCs' perturbation on the smaller domain size (35 members). For the temperature and the geopotential height, the RMSE of the ICs', and LBCs' ensemble is smaller than those of the control run and the ICs' ensemble, as is dispersion. However, the bias (sdbias) of the control run is the smallest (greatest). In other words, the phase error (indicated by dispersion) of the ICs' and LBCs' ensemble is smallest.

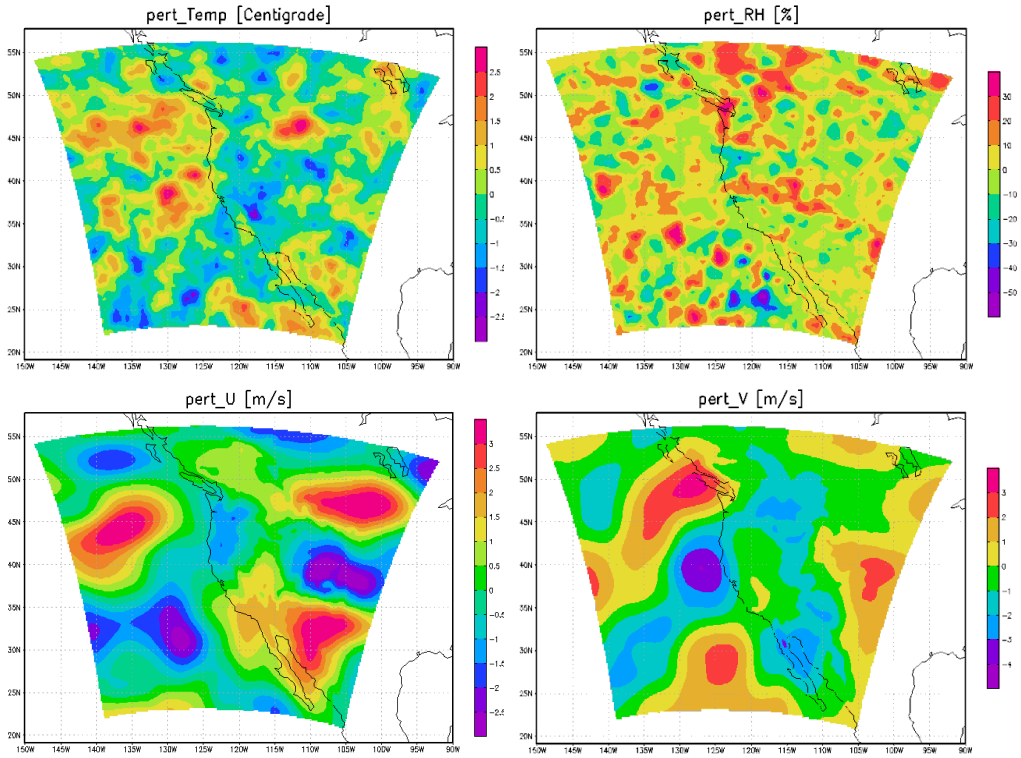

Figure 5. Same as in Fig. 4, but for the nested modeling domain (36 km resolution; shown in Fig. 1).

Another component of the project was to study the predictability of dust storm. Two dust storms originating from the Black Rock Desert (BRD) in northwestern Nevada reaching Fallon within 3-6 hours from the desert significantly reduced visibility less than 10 km are investigated in this study. The large scale dynamic signatures and fine spatial and temporal scale WRF model results showed very promising results and accurate timing of the events compared to the observations at Fallon, NAS and other surface stations in the northwestern NV (Lewis et al. 2010, Kaplan et al. 2010).

Table 2. RMSE (root mean square error), bias, bias of standard deviation (sdbias), and dispersion for the WRF control run, mean of ensemble with IC's perturbation of domain 1 (larger domain), and mean of ensemble of IC's and LBC's perturbation of domain 2 (smaller domain). All results are for the nested domain (domain 2).

	Temperature (°C)			Geopotential Height (gpm)		
	WRF Control	ICs' Ens. Mean	ICs' & LBCs' Ens. Mean	WRF Control	ICs' Ens. Mean	ICs' & LBCs' Ens. Mean
RMSE	5.733	5.719	5.556	130.417	145.714	130.398
Bias	1.766	2.317	2.175	17.459	60.802	29.594
Bias of std.(sdbias)	0.835	0.211	0.626	42.991	27.929	38.676
dispersion	5.495	5.324	5.172	124.491	132.023	123.500

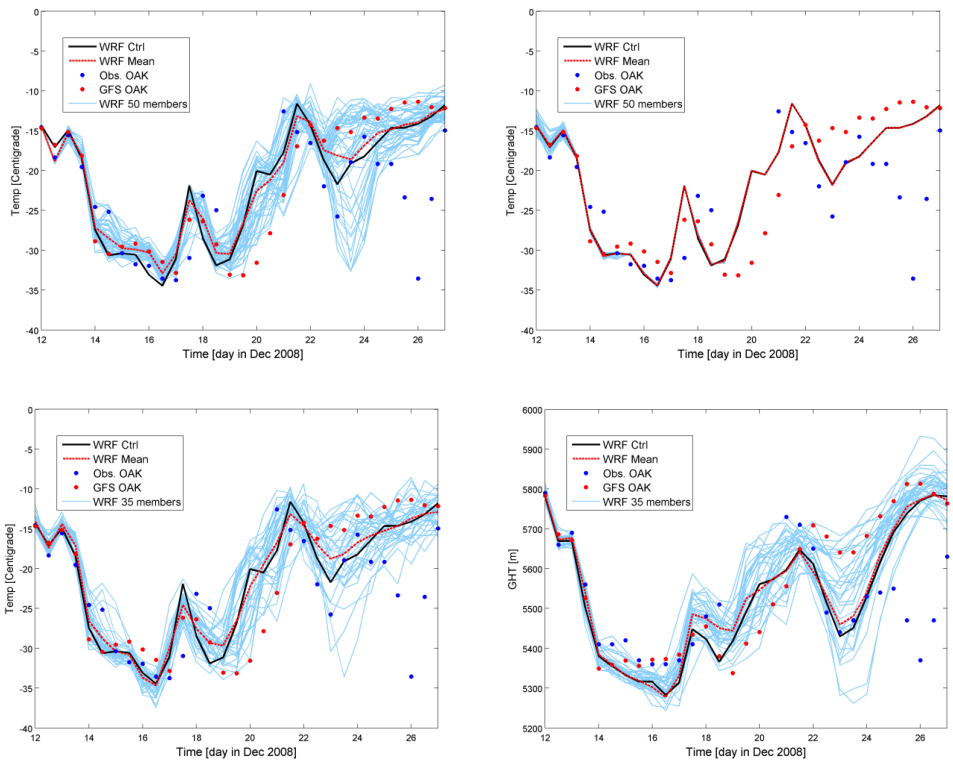

Figure 6. Forecast trajectories of the temperature at 500 hPa (Oakland, CA) with perturbed initial conditions on larger domain size (top left panel; 108 km grid), and from nested domain (top right panel; 36 km grid). Superimposed are radiosonde observations (blue dots), and GFS forecasts (red dots) for the period from 12 to 27 December 2008. The description for the bottom panels are the same as the top panels except for perturbations of the lateral boundary conditions.

IMPACT/APPLICATIONS

Although ensemble forecasting has been used for global predictions at major forecasting centers, regional and mesoscale ensemble forecasting is currently in research and development stage. Furthermore, high-resolution multi-model ensemble forecasting holds promise for regional/mesoscale models' structure through exploration of physical parameterizations that are necessary to improve high-resolution forecasts in complex terrain. Although our research is incomplete, the currently available real time ensemble forecasts are accessible by the Fallon Naval Air Station and will hopefully improve operational nowcasts and forecasts crucial to the Navy's operations.

TRANSITIONS

Both the special set of four weather stations in the Fallon area [http://www.wrcc.dri.edu/] and the ongoing WRF and MM5 operational forecasting system [http://www.adim.dri.edu/] have been developed as a complement to the forecasting and nowcasting at the Navy's Fallon Naval Air Station. The study will also provide guidance for future generation of multi-model ensemble forecasting for the Navy's operations.

RELATED PROJECTS

Dr. Koracin is a co-P.I. on ARO Project entitled "Forecasting of Desert Terrain" where real-time experience and expertise is facilitating an interdisciplinary project linking dust emission modeling, atmospheric predictions and Lagrangian Stochastic Random Particle Dispersion modeling. Dr. Koracin is a Lead Investigator for a Climate Modeling component of the multi-institutional NSF-EPSCoR Project on Climate Change, where they are developing new methods of weather and climate forecasting and use of satellite data assimilation for model evaluation. He is a task leader on another NSF_EPSCoR project for the development of the Cyber-infrastructure and workforce activities. They are also investigating predictability limitations and chaotic behavior in weather and climate predictions and methods of downscaling global model results to regional, mesoscale, and microscale applications. As a Principal Investigator on a DOE-NREL Wind Energy project, he is improving high-resolution forecasts in complex terrain. Dr. Koracin is a Principal Investigator on a DOE-Office of Science project, Simulating Climate on Regional Scale: North Pacific Mesoscale Coupled Air-Ocean Simulations Compared with Observations. The main task is to fully couple the ocean model (POP) and the atmospheric model (WRF) over the open ocean and coastal regions.

Dr. Lewis is involved in two projects that complement this ensemble research; (1) variational analysis used to identify sources of error in dynamical prediction, and (2) analysis and prediction of dust storms over western U.S. Both projects are supported by NOAA and this ONR project.

REFERENCES

Barker, D.M., W. Huang, Y. R. Guo, and Q. N. Xiao., 2004: A Three-Dimensional (3DVAR)Data Assimilation System For Use With MM5: Implementation and Initial Results. Mon. Wea. Rev., 132, 897-914.

Baumhefner, D. P. and D. J. Perkey. Evaluation of lateral boundary errors in a limited-domain model. *Tellus*, 1982, 34, 409-428.

Bayler, G. and H. Lewit , 1992: The Navy Operational Global and Regional Atmospheric Prediction System at the Fleet Numerical Oceanography Center. *Weather and Forecasting*, Vol. 7, No. 2.

Grell, G.A., J. Dudhia and D.R. Stauffer, 1994: *A Description of the Fifth-Generation Penn State/NCAR Mesoscale Model (MM5).* National Center for Atmospheric Research, Techn. Note TN-398, 122 pp.

Hodur, R. M., 1997: The Naval Research Laboratory's Coupled Ocean/Atmosphere Mesoscale Prediction System (COAMPS). *Mon. Wea. Rev*., **125**, 1414-1430.

Hou D., E. Kalnay, and K. K. Drogemeier. Objective Verification of the SAMEX'98 Ensemble Forecast. *Monthly Weather Review*, 2001, 129:73-91.

Houtekamer, P. L., and H. L. Mitchell, 1999: Reply. *Mon. Wea. Rev*., **127**, 1378-1379.

Skamarock, W.C., and Coauthors, 2008: *A description of the Advanced Research WRF Version 3,* NCAR Tech. Note. TN-475+STR, 113 pp. [Available from: http://www.wrf-model.org/wrfadmin/docs/arw_v2.pdf].

Stensrud, D. J., 2001: Using short-range ensemble forecasts for predicting severe weather events. *Atmos. Res.*, **56**, 3-17.

Stensrud, D. J., and S. J. Weiss, 2002: Mesoscale model forecasts of the 3 May 1999 tornado outbreak. *Wea. Forecasting*, **17**, 526-543.

Stensrud, D. J., J.-W. Bao, and T. T. Warner, 2000: Using initial condition and model physics perturbations in short-range ensemble simulations of mesoscale convective systems. *Mon. Wea. Rev*., **128**, 2077-2107.

PUBLICATIONS

Bebis, G., R. D. Boyle, B. Parvin, D. Koracin, Y. Kuno, J. Wang, R. Pajarola, P. Lindstrom, A. Hinkenjann, M.L. Encarnacao, C.T. Silva, D. Coming (Eds.): *Advances in Visual Computing*. 5th International Symposium, ISVC 2009, Las Vegas, NV, USA, 30 November -2 December, 2009. Proceedings, Part I, Lecture Notes in Computer Science, 5876, Springer, 2009, 1117p.

Bebis, G., R. D. Boyle, B. Parvin, D. Koracin, Y. Kuno, J. Wang, R. Pajarola, P. Lindstrom, A. Hinkenjann, M.L. Encarnacao, C.T. Silva, D. Coming (Eds.): *Advances in Visual Computing*. 5th International Symposium, ISVC 2009, Las Vegas, NV, USA, 30 November -2 December, 2009. Proceedings, Part II, Lecture Notes in Computer Science, 5876, Springer, 2009, 1197.

Beg Paklar, G., D. Koracin, and C. Dorman, 2009: Wind-induced ocean circulation along California and Baja California coasts in June 1999. *Atmos. Res.,* **94**, 106-133.

Belu, R., and D. Koracin, 2009: Wind characteristics and wind energy potential in western Nevada. *Renewable Energy*, **34**, 2246-2251.

Chen, L.-W.A., D. Lowenthal, J.G. Watson, D. Koracin, D. Dubois, R. Vellore, N. Kumar, E.M. Knipping, N. Wheeler, K. Craig, S. Reid, 2010: Factors or sources: investigation of multivariate receptor modeling with simulated PM2.5 data. *J. Air & Waste Manage. Assoc.*, **60**, 43-54.

Horvath, K., D. Koracin, R. Vellore, A. Bajic, R. Belu, and T. McCord (2009): Sub-kilometer dynamical downscaling over complex terrain: Does a refinement of horizontal resolution uniquely bring increasing the model accuracy? *American Geophysical Union Annual Meeting*, San Francisco, CA, 14-18 December 2009.

Kaplan, M., R. Vellore, and J. Lewis, 2010: Dust storm over the Black Rock Desert: Sub-synoptic analysis of unbalanced circulations across the jet streak. Submitted to the *J. Geophy. Res.* (Atmospheres).

Koracin, D., R. Vellore, D. H. Lowenthal, J. G. Watson, J. Koracin, T. McCord, D. W. DuBois, and L.-W. Antony Chen, 2010: Regional source identification using lagrangian stochastic particle dispersion and HYSPLIT backward-trajectory models. *J. Air & Waste Manage. Assoc. (in review).*

Koračin, D., R. Vellore, J. Lewis, and M. Kaplan (2009): Predictability of coastal weather and its implications to ensemble forecasting, Eighth Conference on Coastal Atmospheric and Oceanic Prediction and Processes, *89th American Meteorological Society Meeting*, 11-15 January 2009, Phoenix, Arizona.

Koracin, D. and R. Vellore (2009): Predictions of the west coast climate using dynamical downscaling. *34th Annual Climate Diagnostics and Prediction Workshop*, Monterey, CA, October 26-30, 2009.

Koracin, D., R. Vellore, B. Hatchett, J. Kahyaoglu-Koracin, K. Horvath, and R. Belu, (2009). Variability of climate predictions relevant to hydrological resources. *American Geophysical Union Annual Meeting*, San Francisco, CA, 14-18 December 2009.

Lakshmivarahan, S., and J. Lewis, 2009: Forward sensitivity approach to dynamic data assimilation. *Advances in Meteorology*, doi:10.1155/2010/375615.

Lewis, J., M. Kaplan, R. Vellore, R. Rabin, J. Hallett, and S. Cohn, 2010: Dust storm over the Black Rock Desert: Large scale dynamic signatures. *J. Geophy. Res., (Accepted).*

Lowenthal, D. H., J. G. Watson, D. Koracin, L.-W. A. Chen, D. Dubois, R. Vellore, N. Kumar, E. M. Knipping, N. Wheeler, K. Craig, and S. Reid, 2010: Evaluation of regional scale receptor modeling. *J. Air & Waste Manage. Assoc.*, **60**, 26-42.

McAlpine, J.D., D. Koracin, D. P. Boyle, J. A. Gillies, and E. V. McDonald, 2010: Development of a rotorcraft dust-emission parameterization using a CFD model. *Environ. Fluid Mechan. (in print).*

Zabkar, R., J. Rakovec, and D. Koracin, 2010: The roles of regional accumulation and advection of ozone during high ozone episodes in Slovenia: a WRF/Chem modelling study. *Atmos. Environ. (in print).*